Chemical Science

ROYAL SOCIETY OF CHEMISTRY

EDGE ARTICLE

View Article Online
View Journal | View Issue

Cite this: *Chem. Sci.*, 2022, **13**, 1298

All publication charges for this article have been paid for by the Royal Society of Chemistry

Received 10th December 2021
Accepted 13th January 2022

DOI: 10.1039/d1sc06907a

rsc.li/chemical-science

C(sp^3)–H oxygenation *via* alkoxypalladium(II) species: an update for the mechanism†

Shuaizhong Zhang,‡ Jinquan Zhang ‡ and Hongbin Zou *

Pd-catalyzed C(sp^3)–H oxygenation has emerged as an attractive strategy for organic synthesis. The most commonly proposed mechanism involves C(sp^3)–H activation followed by oxidative addition of an oxygen electrophile to give an alkylpalladium(IV) species and further C(sp^3)–O reductive elimination. In the present study of γ-C(sp^3)–H acyloxylation of amine derivatives, we show a different mechanism when *tert*-butyl hydroperoxide (TBHP) is used as an oxidant—namely, a bimetallic oxidative addition-oxo-insertion process. This catalytic model results in an alkoxypalladium(II) intermediate from which acyloxylation and alkoxylation products are formed. Experimental and computational studies, including isolation of the putative post-oxo-insertion alkoxypalladium(II) intermediates, support this mechanistic model. Density functional theory reveals that the classical alkylpalladium(IV) oxidative addition pathway is higher in energy than the bimetallic oxo-insertion pathway. Further kinetic studies revealed second-order dependence on [Pd] and first-order on [TBHP], which is consistent with DFT analysis. This procedure is compatible with a wide range of acids and alcohols for γ-C(sp^3)–H oxygenation. Preliminary functional group transformations of the products underscore the great potential of this protocol for structural manipulation.

Introduction

The development of approaches for direct C–O formation of unactivated C(sp^3)–H remains a fundamental challenge in synthetic chemistry owing to the high bond dissociation energy of the aliphatic C–H bonds; solving this problem is highly desirable considering the great manipulation potential of organic compounds.[1] In the past decade, Pd-catalyzed C(sp^3)–H oxygenation has been proven to be a promising way to tackle this challenge through a combination of various oxidants such as PhI(OAc)$_2$,[2] $K_2S_2O_8$,[3] and *N*-fluoropyridinium[4] (Scheme 1a). In 2004, Canty's group reported the generation of the ^{1}H NMR-detectable alkylpalladium(IV) intermediate ($Pd^{IV}(O_2CPh)_2Me_2(L_2)$) from $Pd^{II}Me_2(L_2)$ using $(PhCO)_2O_2$ as an oxidant.[5] This system could deliver the corresponding product with a newly formed C–O bond after decomposition. Following this observation, subsequent Pd-catalyzed C(sp^3)–H oxygenation studies continuously proposed that these transformations undergo oxidative addition of an oxygen electrophile to give an alkylpalladium(IV) (C(sp^3)–[Pd(IV)(L_n)]–O) species, which further proceeds through C(sp^3)–O reductive elimination to give the oxidized products (Scheme 1a). In 2004, the Sanford laboratory demonstrated that PhI(OAc)$_2$ was an effective oxidant that facilitated formation of an alkylpalladium(IV) species affording C(sp^3)–H acetoxylation products.[6] In addition to the most widely used oxidant PhI(OAc)$_2$, peroxides such as MeCOOO^{t}Bu and *tert*-butyl hydroperoxide (TBHP) also serve as alternative efficient oxidants for C(sp^3)–H oxygenation. In 2005, Yu's group pioneered the use of peroxide MeCOOO^{t}Bu for oxazoline-directed β-C(sp^3)–H acetoxylation, and the alkylpalladium(IV) complex was speculated to be the reaction intermediate.[7] Recently, Yu *et al.* employed TBHP to realize the β-C(sp^3)–H lactonization[8] or acetoxylation[9] of free acid *via* speculated

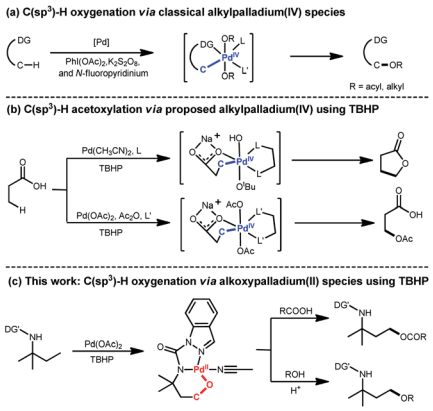

Scheme 1 C–H oxygenation with different Pd intermediates.

College of Pharmaceutical Sciences, Zhejiang University, Hangzhou, Zhejiang, 310058, P. R. China. E-mail: zouhb@zju.edu.cn

† Electronic supplementary information (ESI) available: Experimental details, synthetic procedures, characterization data and NMR spectra. CCDC 2058762 (**IN14**). For ESI and crystallographic data in CIF or other electronic format see DOI: 10.1039/d1sc06907a

‡ These authors contributed equally to this work.

alkylpalladium(IV) species (Scheme 1b). Despite this progress toward unactivated C(sp^3)–H oxygenation, the catalytic mechanism is still unclear owing to the absence of catalytically relevant palladacycle complexes.

Herein, we show the Pd-catalyzed γ-C(sp^3)–H oxygenation of *tert*-amylamine (**1a**) *via* unexpected alkoxypalladium(II) (C(sp^3)–O–[Pd(II)(L_n)]) species using TBHP as the oxidant (Scheme 1c). This interesting finding—together with van Koten's pioneering discovery of C(sp^2)–O–[Pd(II)(L_n)] species[10] in the presence of TBHP—prompted us to gain insights into this transformation. Experimental and computational studies were hence combined to investigate a plausible reaction mechanism, including the isolation of alkoxypalladium(II) intermediates, density functional theory (DFT) calculations, and further kinetic studies. In addition, a wide range of carboxylic acids, N-protected amino acids, and carboxyl-containing drugs were tested to understand the substrate scope of the unactivated γ-C(sp^3)–H acyloxylation as well as the alcohols' scope within γ-C(sp^3)–H alkoxylation *via* the assistance of H^+.

Results and discussion

Our initial studies began with the γ-C(sp^3)–H acyloxylation of *N*-(*tert*-pentyl)-1*H*-indazole-1-carboxamide (**1a**) by testing a wide range of reaction parameters, including oxidants, solvents, and temperature (Table 1, refer Tables S1 and S2 in the ESI† for detailed reaction condition screening). Treating **1a** with benzoic acid (**2a**) in the presence of $Pd(OAc)_2$ and *N*-flouro-2,4,6-trimethylpyridinium tetraflouroborate ($[F^+]BF_4^-$) in hexafluoroisopropanol (HFIP) at 45 °C for 36 h provided the desired C(sp^3)–H acyloxylation product **3a** with an isolated yield of 18% (entry 1). Replacing the oxidant with TBHP (5 M in decane) boosted the yield of **3a** to 55% (entry 2), while TBHP (70% in water) further increased the yield to 68% (entry 3). Other peroxide oxidants such as cumene hydroperoxide (CHP) and MeCOOO^{t}Bu could also drive this reaction with lower yields

Table 1 Optimization of acyloxylation reaction conditions[a]

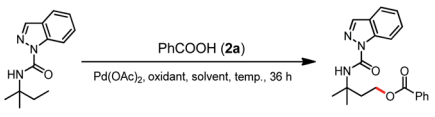

Entry	Oxidant	Solvent	Temp (°C)	Yield[b] (%)
1	$[F^+]BF_4^-$	HFIP	45	18
2	TBHP (5 M in decane)	HFIP	45	55
3	TBHP (70% in water)	HFIP	45	68
4	CHP	HFIP	45	23
5	MeCOOO^{t}Bu	HFIP	45	26
6	TBHP (70% in water)	Toluene	45	20
7	**TBHP (70% in water)**	**CH_3CN**	**45**	77

[a] For entries 1–7: reaction was conducted with **1a** (0.2 mmol), **2a** (0.6 mmol), $Pd(OAc)_2$ (0.02 mmol), oxidant (0.6 mmol) and solvent (1 mL). [b] Isolated yield.

Table 2 Optimization of alkoxylation reaction conditions[a]

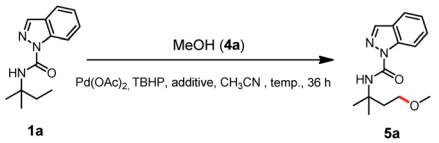

Entry	Solvent	Additive	Temp (°C)	Yield[b] (%)
1	CH_3CN	—	45	24
2	CH_3CN	AcOH	45	39
3	CH_3CN	TFA	45	48
4	**CH_3CN**	**TFA**	**60**	**71**
5	CH_3CN	TFA	80	43
6[c]	CH_3CN	TFA	45	60

[a] For entries 1–6: reaction was conducted with **1a** (0.2 mmol), **4a** (1.0 mmol), $Pd(OAc)_2$ (0.02 mol), oxidant (0.6 mmol), additive (5 μL) and solvent (1 mL). [b] Isolated yield. [c] Additive (10 μL).

(entries 4 and 5); TBHP (70% in water) was identified as the choice of oxidant (entry 3). Further solvent screening (entries 6 and 7) showed that entry 7 (acetonitrile solvent) contained the most favorable reaction conditions to afford **3a** with an elevated yield of 77%.

With the optimal γ-C(sp^3)–H acyloxylation of **1a** established, we next show that simple replacement of benzoic acid with methanol (**4a**) resulted in the exclusive alkoxylation product **5a** with a 24% yield (entry 1, Table 2). Acid additive screening showed that 0.5% acetic acid (AcOH) increased the yield to 39% (entry 2), while 0.5% CF_3COOH (TFA) further improved the yield to 48% (entry 3). The reaction temperature was also tested, and the results (entries 3–5) indicated that 60 °C was optimal for **5a** formation with a yield of 71%. Further addition of TFA was also tested with a decreased yield of **5a** (60%, entry 6). Hence, entry 4 was the best choice for γ-C(sp^3)–H alkoxylation of **1a**.

Encouraged by the selective γ-C(sp^3)–H acyloxylation and alkoxylation findings, we next performed stoichiometric reactions to investigate the reaction intermediates. Exposing *N*-(*tert*-pentyl)-1*H*-indazole-1-carboxamide (**1a**) to $Pd(OAc)_2$ in MeCN at room temperature in the presence of TBHP afforded the corresponding mono [5, 6]-fused palladacycle **IN17**. Replacement of MeCN with AcOH/MeCN (2%, w/w) exclusively resulted in another palladacycle **IN14** under otherwise similar reaction conditions (Scheme 2a). Fortunately, the intermediate **IN14** was isolated, and its structure was confirmed by X-ray crystallography to be a [5, 6]-fused palladacycle dimer (**IN14**, CCDC: 2058762†) (Scheme 2a). Intrigued by the discovery of **IN14** and **IN17**, a [5, 5]-fused palladacycle **IN6** was also isolated by treating **1a** with $Pd(OAc)_2$ in AcOH/MeCN (w/w, 2%) solvent at room temperature.

Previously, alkylpalladium(IV) species were reported to be the classical reaction intermediates for C(sp^3)–H oxygenation, and a similar mechanism was proposed in Pd-catalyzed β-C(sp^3)–H oxygenation using TBHP as the coupling oxidant. Contrary to these general findings, the alkoxypalladium(II) species (**IN14** and **IN17**) were surprisingly found here. This led us to consider three fascinating questions: (1) Are the alkoxypalladium(II)

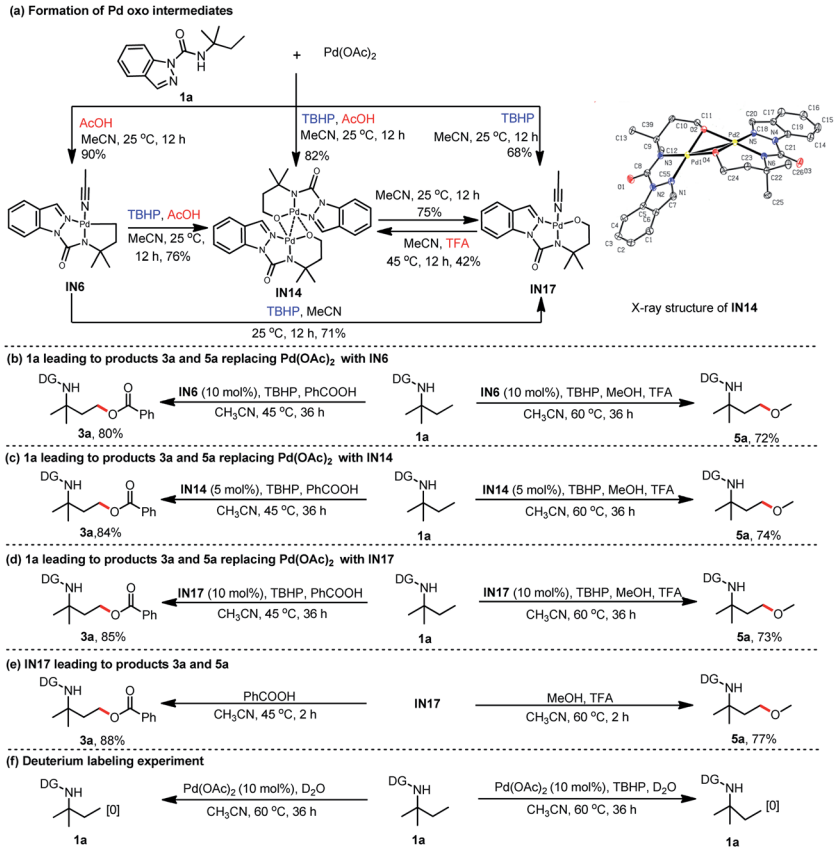

Scheme 2 Mechanistic studies.

species **IN14** and **IN17** the real reaction intermediates for this C(sp^3)–H oxygenation? (2) Why does this C(sp^3)–H oxygenation process prefer the alkoxypalladium(II) species rather than the alkylpalladium(IV) species? (3) What is the possible reaction process to afford the alkoxypalladium(II) species?

Additional experiments were conducted to confirm the role of these isolated intermediates. As expected, a catalytic amount of **IN6** was used to replace $Pd(OAc)_2$, thus affording **3a** and **5a** with 80% and 72% yields, respectively (Scheme 2b). **IN6** could be readily transformed to **IN14** or **IN17** with the assistance of TBHP in AcOH/MeCN (w/w, 2%) or MeCN, respectively. Interestingly, the conversion between **IN14** and

IN17 in the corresponding solvent was also observed (Scheme 2a). Similar treatment of **1a** with **IN14** delivered products **3a** and **5a** in 84% and 74% yields, respectively (Scheme 2c). Reaction of **1a** with **IN17** also gave **3a** (85%) and **5a** (73%) (Scheme 2d). These findings suggest that **IN6**, **IN14**, and **IN17** are catalytically relevant intermediates in the synthetic process for the desired γ-C(sp^3)–H oxygenation products. Direct treatment of **IN17** with PhCOOH and MeOH resulted in higher production yields of **3a** (88%) and **5a** (77%) (Scheme 2e). This result further indicates that this γ-C(sp^3)–H oxidative transformation goes through the alkoxypalladium(II) species. Deuterium incorporation experiments of **1a** were also investigated, and the results indicate that the C(sp^3)–H insertion process is irreversible because no deuterium-labeled **1a** was observed (Scheme 2f).

To address questions 2 and 3 more specifically, computational experiments were conducted using DFT calculations *via* the M062x method[11] with Gaussian 16 program suite[12] (refer ESI† for computational details). First, the generation of a [5, 5]-fused palladacycle **IN6** was studied. This progress starts with the coordination of **1a** with $Pd(OAc)_2$ to form a five-membered palladacycle **IN3** *via* **TS1** and **TS2** with activation free energies of 17.1 and 5.7 kcal mol^{-1}, respectively (Fig. 1). The subsequent γ-C(sp^3)–H activation occurs next to obtain the [5, 5]-fused palladacycle **IN5** *via* **TS3** and **TS4** with activation free energies of 9.0 and 12.6 kcal mol^{-1}, respectively. MeCN was considered to be a coordinating solvent, and the MeCN-coordinated intermediate **IN6** was obtained *via* **TS5** with an energy barrier of 4.9 kcal mol^{-1}. The overall free energy barrier of the C–H cleavage transition state was 20.8 kcal mol^{-1} (from **IN3** to **TS4**).

After the generation of the activation intermediate **IN6**, we next investigated the possibility of alkylpalladium(IV) species (**IN8**) formation based on previously reported general mechanisms. This assumption is outlined in blue, and the palladium complex **IN6** from **1a** was used to simplify the computations (Fig. 2). The coordination of TBHP to **IN6** results in **IN7** with an energy barrier of 6.2 kcal mol^{-1}—this subsequently transforms to the resulting alkylpalladium(IV) intermediate **IN8** *via* **TS6** with an activation free energy of 84.6 kcal mol^{-1}. This extremely high free energy barrier indicates that **IN8** is not favorable for our reaction, and it may not be relevant in the catalytic cycle.

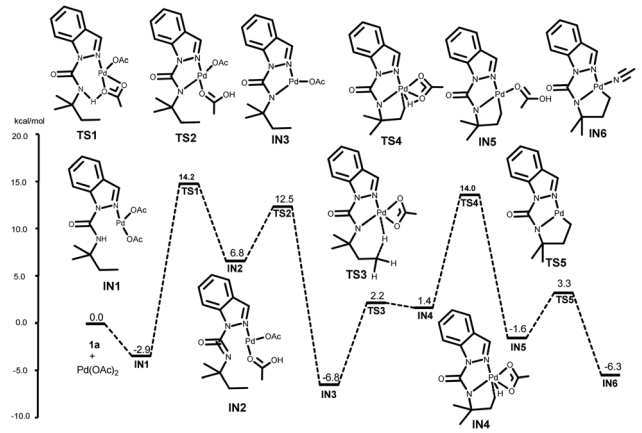

Fig. 1 Free energy profiles (kcal mol^{-1}) of C–H activation.

We then turned our attention to determining a plausible pathway from **IN6** to **IN17** and two approaches were proposed (black and red lines, Fig. 2). The black line shows the hypothesis that the dimeric palladacycles undergo the entire reaction pathway. As shown by previous reports on bimetallic intermediate formation in C(sp^2)–H activation,[13] this reaction could also begin with the generation of the dimeric Pd(II) intermediate **IN9** from **IN6** with an energy barrier of 9.9 kcal mol^{-1}. The coordination of TBHP to **IN9** leads to complex **IN10**. **IN10** further undergoes oxidative addition of the O–O bond of TBHP *via* **TS7** to generate **IN11**, and **IN11** follows the same pathway to obtain Pd(IV) intermediate **IN12** *via* **TS8** with activation free energies of 42.6 and 32.7 kcal mol^{-1}, respectively. **IN13** is subsequently obtained *via* C–O bond formation from **IN12** *via* **TS9**. The desired alkoxypalladium(II) intermediate **IN14** is achieved by repeating the same pathway with activation barriers of 2.1 and 2.2 kcal mol^{-1}, respectively. Next, the MeCN-coordinated form intermediate **IN16** is formed by the release of weak interaction between Pd and O (*via* **TS11** and **IN15**) with the assistance of MeCN and an energy barrier of 25.0 kcal mol^{-1}. Finally, two MeCN-coordinated intermediates **IN17** are formed by repeating this process. The overall free energy barrier of this process is 45.3 kcal mol^{-1} (from **IN6** to **TS7**).

Alternatively, the red line represents a process that involves direct development of the monomer palladacycle complex **IN7** to the alkoxypalladium(II) intermediate **IN17**. **IN7** goes through an oxidative reaction to form **IN18** *via* **TS13** with an energy barrier of 53.4 kcal mol^{-1}. Subsequent MeCN coordination affords intermediate **IN19**. However, the overall free energy barrier is 59.6 kcal mol^{-1} (from **IN6** to **TS13**). The results showed that the bimetallic oxidative addition-oxo-insertion pathway is energetically feasible due to its lower energy barrier than the other two potential processes.

The aforementioned computational calculation results indicated that the oxidative addition progress is likely the turnover-limiting step. As described by Blackmond,[14] reaction progress kinetic analysis is a simple, systematic method to obtain a complete picture of a reaction's kinetic profile. **1a** and **2aa** were

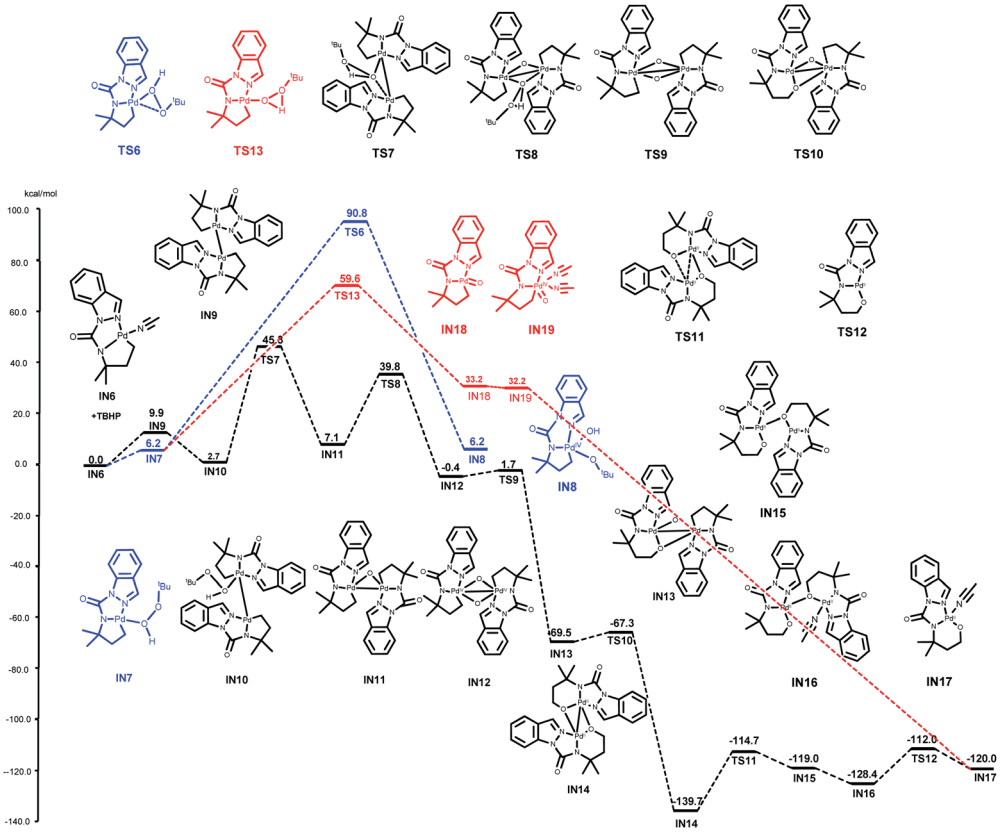

Fig. 2 Free energy profiles (kcal mol^{-1}) of oxidative addition.

used to investigate the dependence of the reaction rate. Reaction rate comparisons between the standard initial condition and higher [**1a**] or lower [**2aa**] conditions show zero-order dependence in [**1a**] or [**2aa**]. These results indicate that **1a** or [**2aa**] is irrelevant to the rate-determining step of this catalytic cycle. However, lower concentration of [Oxidant] or higher concentration of [Pd] led to a lower or higher reaction rate, respectively, suggesting a positive-order dependence on [Oxidant] and [Pd] (refer ESI Section 6.1†). The dependence of the reaction rates on [Pd] and [TBHP] was also comprehensively investigated (refer ESI Sections 6.2 and 6.3†). A first-order with respect to [TBHP] and a second-order dependence at low [Pd] were observed (Scheme 3), which is consistent with DFT analysis.

Based on the experimental and computational observations, a plausible C(sp^3)–H oxygenation mechanism *via* the alkoxypalladium(II) species is proposed using **3aa** as an example (Scheme 4). The initial coordination of **1a** with $Pd(OAc)_2$ and MeCN gives the [5, 5]-fused monomer Pd(II) intermediate **IN6**. A subsequent dimeric Pd(II) intermediate **IN9** is formed by the release of two coordinated MeCN molecules and the following formation of a weak interaction between Pd. Next, the oxidative addition of **IN9** by TBHP provides oxenoid oxygen atoms and oxygen insertion into the Pd–C bond gives the dimeric alkoxypalladium(II) intermediate **IN14**. The MeCN-coordinated monomer alkoxypalladium(II) intermediate **IN17** is then promoted by the release of a weak interaction between Pd and O and the formation of the Pd–N (MeCN) bond. Two possible pathways[15] from **IN17** are proposed to generate the oxygenation product: (1) oxidative addition of **IN17** produces LPd(IV)$(OAc)_2$(OR) species and further reductive elimination yields **3aa.** However, this pathway was ruled out because we found that direct treatment of **IN17** with PhCOOH and MeOH resulted in the acyloxylation and alkoxylation products (Scheme 2e). (2) AcOH is engaged in bonding with the Pd and C center to generate **IN20** and subsequent elimination generates **IN21**, that is redox-neutral at the Pd(II) center. Final proto-depalladation of **IN21** in the presence of two additional equivalents of HOAc yields **3aa** and regenerates $Pd(OAc)_2$ to continuously drive the catalytic cycle.

With the optimized reaction conditions of γ-C(sp^3)–H oxygenation in hand (Table 1, entry 7 and Table 2, entry 4), we first investigated the carboxylic acid scope of the acyloxylation reaction (Scheme 5). Various mono-substituted benzoic acids including fluorine, chlorine, bromine, trifluoromethyl, cyano, nitro, methyl, underwent the desired acyloxylation reaction in moderate to excellent isolated yields ranging from 57% to 92% (**3a–3n**). The results also showed that the electron-withdrawing group (**3b–3f**) at the *para* position on the phenyl ring was preferable to those with an electron-donating group (**3h**, **3i**) except for the acetyl group (**3g**). This observation could also be extended to substituents at the *meta* or *ortho* positions in which the electron-withdrawing chloro (**3j**, **3m**) or nitro group (**3k**) were superior to the electron-donating methyl (**3l**) or methoxy (**3n**) group. The same trends were also recorded for the disubstituted benzoic acids—the chloro groups (**3o**, **3q**) had more turnover than their corresponding methyl groups (**3p**, **3r**). Meanwhile, more sterically hindered diphenyl-, naphthyl-, and (methylenedioxy)phenyl-substituted acids gave relatively lower yields (**3s–3u**). Other aromatic acids containing substituted pyridines, thiophene, and indole were all compatible coupling partners, thus providing products in moderate isolated yields (36–63%, **3v–3y**). The substrate scope of aliphatic acids was also investigated (Scheme 5). Primary aliphatic acids including acetic acid (**3aa**), propionic acid (**3ab**), isovaleric acid (**3ac**), neovaleric acid (**3ad**), and hexanoic acid (**3ae**) were well tolerated in the C(sp^3)–H acyloxylation reaction with good isolated

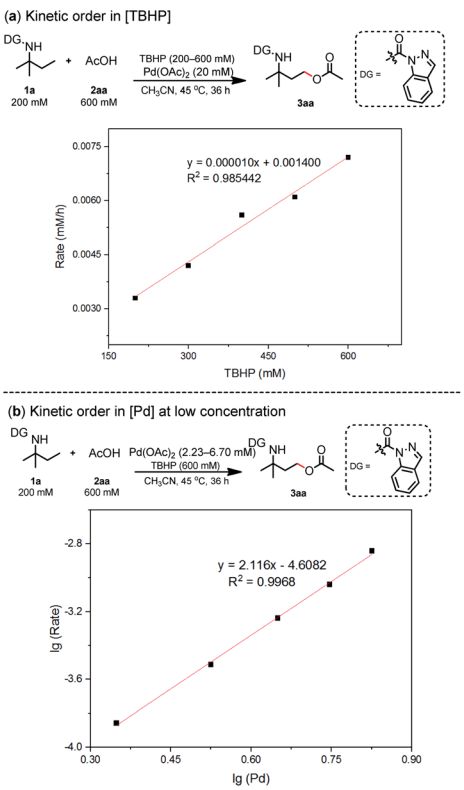

Scheme 3 Kinetic studies.

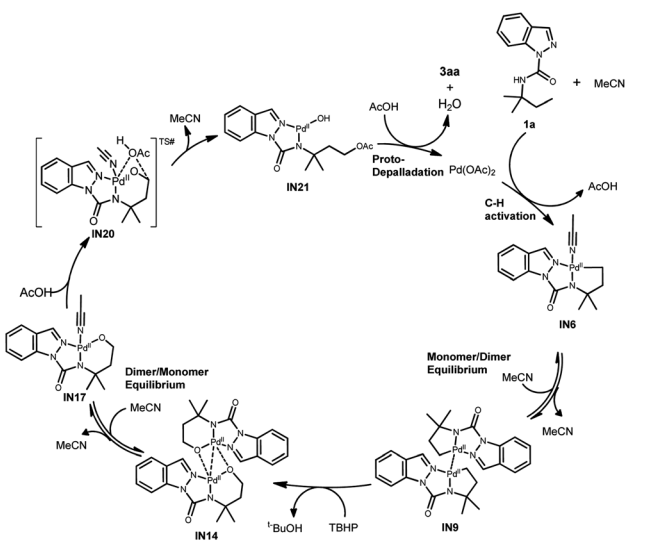

Scheme 4 Proposed mechanism.

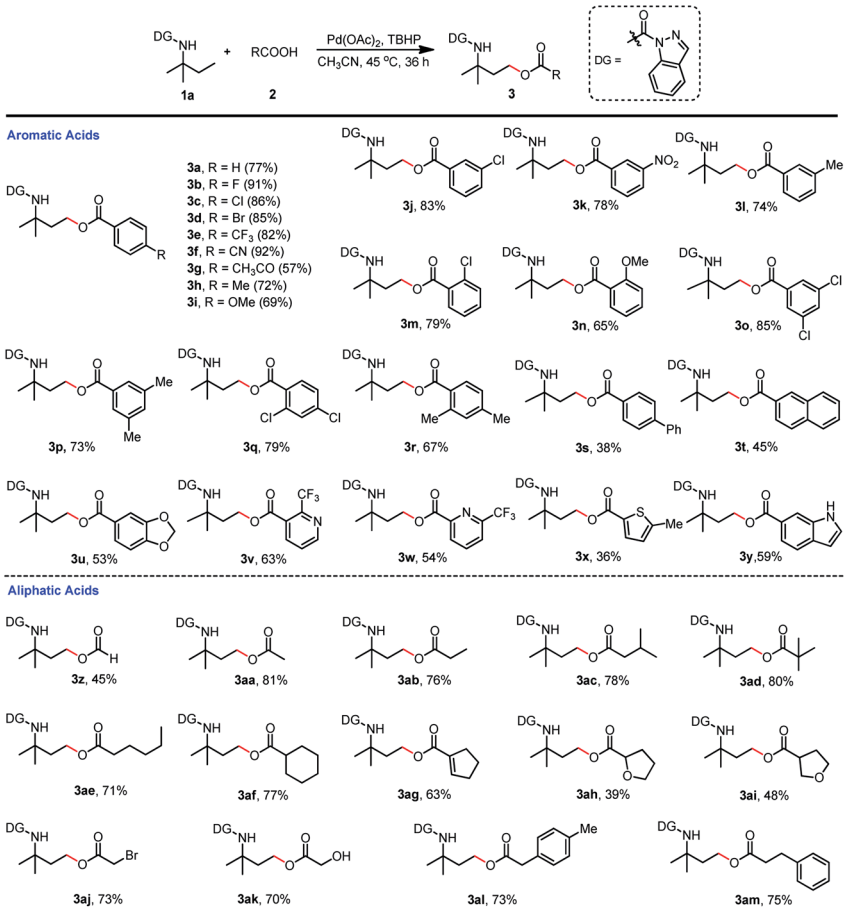

Scheme 5 Scope of carboxylic acids for γ-C(sp^3)–H acyloxylation. (a) Reaction was conducted with **1a** (0.2 mmol), **2** (0.6 mmol), $Pd(OAc)_2$ (0.02 mmol), TBHP (70% in water) (0.6 mmol) and CH_3CN (1 mL) at 45 °C for 36 h. (b) Isolated yield.

yields (71–81%); formic acid achieved a relatively lower efficiency (**3z**). Saturated (**3af**) or unsaturated (**3ag**) secondary aliphatic acids also successfully led to the products with high efficiency. Aliphatic acids with oxygenated functionalities (**3ah**, **3ai**) or reactive bromine or hydroxyl groups (**3aj**, **3ak**) at the alpha sites were amenable to this transformation, thus affording the targeted products in moderate-to-good isolated yields. Aralkyl group-substituted aliphatic acids could also be efficiently converted to the desired products **3al** and **3am** with 73% and 75% isolated yields, respectively.

This protocol could also be well adapted for N-Boc-protected amino acids such as Boc-glycine, Boc-β-alanine, Boc-L-phenylalanine, Boc-L-isoleucine, Boc-D-valine, and Boc-L-threonine to afford the corresponding products (**3an–3as**) with isolated yields of 61–75% (Scheme 6). Meanwhile, acetyl-L-phenylalanine was also tested to give **3at** with a relatively lower yield of 36%, and a higher reaction temperature treatment of Boc-protected tripeptide resulted in the desired product **3au** with a slightly lower yield of 33%. These results broadly enhanced the palladium catalyzed γ-C(sp^3)–H acyloxylation capabilities and provide a new approach for amino acid derivatization.

Encouraged by these outcomes, we next tested the applicability of this method for the esterification of drugs containing

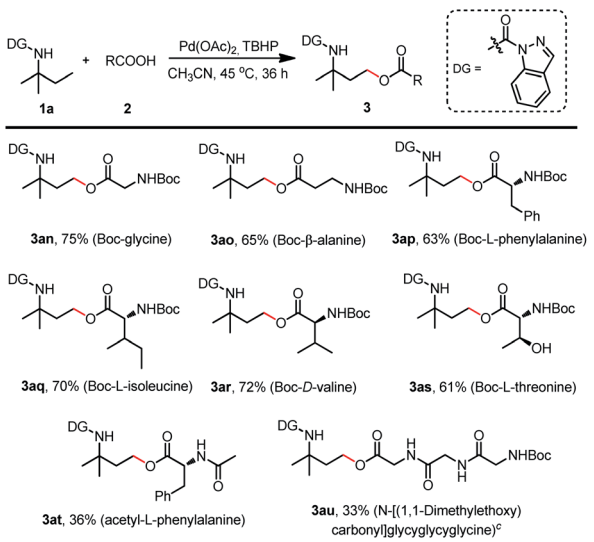

Scheme 6 Scope of N-protected amino acids. (a) Reaction was conducted with **1a** (0.2 mmol), **2** (0.6 mmol), $Pd(OAc)_2$ (0.02 mmol), TBHP (70% in water) (0.6 mmol) and CH_3CN (1 mL) at 45 °C for 36 h. (b) Isolated yield. [c]Reaction was conducted at 60 °C.

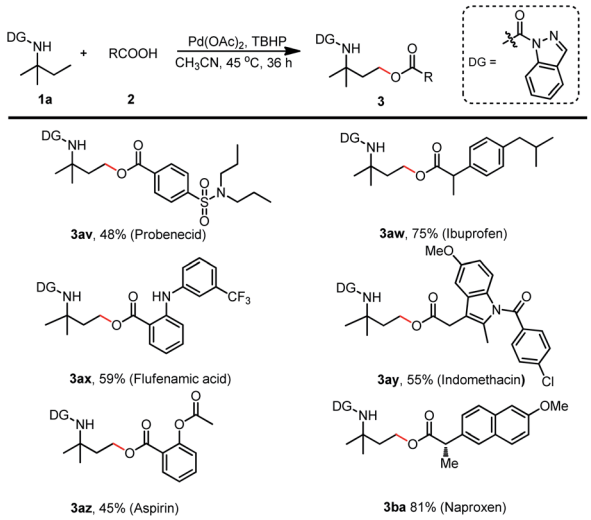

Scheme 7 Scope of drugs for esterification. (a) Reaction was conducted with **1a** (0.2 mmol), **2** (0.6 mmol), $Pd(OAc)_2$ (0.02 mmol), TBHP (70% in water) (0.6 mmol) and CH_3CN (1 mL) at 45 °C for 36 h. (b) Isolated yield.

acid moieties (Scheme 7). Probenecid, ibuprofen, flufenamic acid, indomethacin, aspirin, and naproxen resulted in the desired products (**3av–3ba**) in moderate to good yields (45% to 81%). These findings further demonstrated this protocol's potential to perform late-stage facile functionalization and generate amine-containing drug analogs.

Schemes 5–7 show that a variety of carboxylic acids were tolerated during the γ-acyloxylation of **1a**. With the optimal reaction conditions for **1a** γ-alkoxylation in hand (Table 2, entry 4), different alcohols were tested for the substrate scope (Scheme 8). Primary alcohols such as methanol, deuterated methanol, ethanol, *n*-propanol, *n*-butanol, *n*-pentanol, *n*-octanol, and cyclopentylmethanol successfully afforded the desired alkoxylation products with 45–71% isolated yields (**5a–5g**).

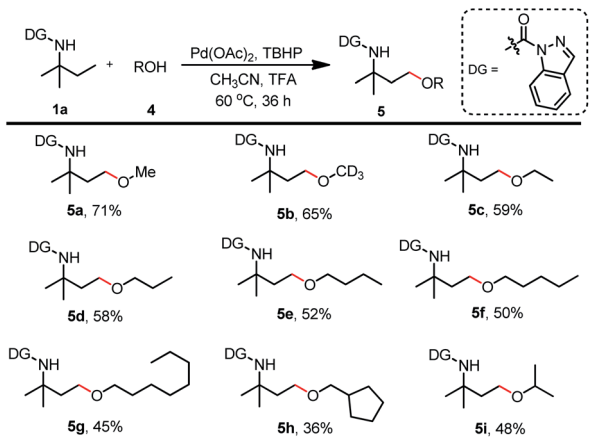

Scheme 8 Scope of natural products for $C(sp^3)$–H alkoxylation. (a) Reaction was conducted with **1a** (0.2 mmol), **4** (1.0 mmol), $Pd(OAc)_2$ (0.02 mmol), TBHP (70% in water) (0.6 mmol), TFA (5 μL) and CH_3CN (1 mL) at 60 °C for 36 h. (b) Isolated yield.

Secondary alcohols such as isopropanol and cyclohexanol were also acceptable for this transformation with moderate isolated yields (**5h**, **5i**).

A scaled up (2.0 mmol) oxygenation reaction of **1a** was conducted to demonstrate the synthetic utility of this newly developed approach (Scheme 9). Products **3a** and **5a** were afforded with isolated yields of 54% and 48%, respectively. Increasing the reaction time to 60 h gave a higher yield of **3a** (65%) and **5a** (54%), thus showing the good efficiency of our protocol (Scheme 9a). Moreover, directing group (DG) deprotection of **3a** and **5a** *via* hydrolysis was accompanied by ester bond breakage to deliver a hydroxyl derivative that underwent an *in situ* one-pot benzoyl protection process to yield the Bz-protected **6** for easy purification and analysis. Hence, removal of DG from **3a** led to amino alcohol derivative **6** with 68% yield. Applying the same strategy to **5a** resulted in the amino ether derivative **7** with a 72% yield. The partial hydrolysis of the ester bond could also be realized, and product **3h** was easily converted into the corresponding primary alcohol **8** with an 89% yield (Scheme 9b). Treatment of **8** with azidotrimethylsilane ($TMSN_3$) and $Bi(OTf)_3$ enabled the formation of **9** with a 68% yield while *N*-bromosuccinimide (NBS) and dimethylthiourea (DMTU) treatment easily converted the hydroxy group of **8** to a reactive functional bromine group (**10**) with an 82% yield. Meanwhile, after dealing with 2,3-dichloro-5,6-dicyano-1,4-benzoquinone (DDQ), PPh_3, and *n*-Bu_4NCN, the hydroxyl group of **8** could also be transformed to the cyano group (**11**) with a 54% yield (Scheme 9b). These transformations demonstrate the great potential of the

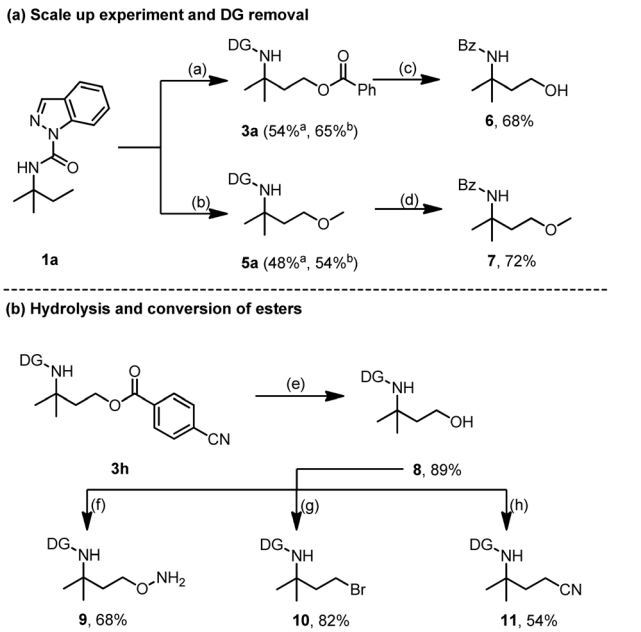

Scheme 9 Synthetic applications. Legend: (a) $Pd(OAc)_2$, PhCOOH, TBHP, CH_3CN, 45 °C; (b) $Pd(OAc)_2$, MeOH, TFA, TBHP, CH_3CN, 60 °C; (c) K_2CO_3, MeOH, H_2O, BzCl, 68%; (d) K_2CO_3, MeOH, H_2O, BzCl, 72%; (e) LiOH, THF, H_2O, 89%; (f) $TMSN_3$, $Bi(OTf)_3$, CH_3NO_2, 68%; (g) NBS, DMTU, CH_2Cl_2, 82%; (h) DDQ, PPh_3, *n*-Bu_4NCN, CH_3CN, 54%. [a]Standard reaction condition. [b]Reaction was conducted for 60 h.

selective C(sp^3)–H acyloxylation and alkoxylation for facile access to amine-containing functional molecules.

Conclusions

In summary, we developed a general method for γ-C(sp^3)–H acyloxylation and alkoxylation of *tert*-amylamine using 1*H*-indazole as the directing group and TBHP (70% in water) as an inexpensive oxidant. Unexpectedly, the alkoxypalladium(II) intermediate **IN17** was captured, which goes through a SN_2 process that is redox-neutral at the Pd(II) center to afford the oxygenation products. To the best of our knowledge, this is the first time that C(sp^3)–H oxygenation is realized through a C(sp^3)–O–[Pd(II)(Ln)] species in contrast to the classical proposed catalytic pathway with alkylpalladium(IV) species. Experimental and computational experiments were performed to study the reaction mechanism. Two alkoxypalladium(II) intermediates (**IN14** and **IN17**) were isolated and characterized. The DFT calculations showed the preference for the addition-oxo-insertion process with lower energy. The results also revealed that **IN17** is generated through a bimetallic oxo-insertion pathway as confirmed by kinetic studies. The results provide an update to the underlying reaction mechanism of palladium-catalyzed oxidative C(sp^3)–H oxygenation especially for peroxide-assisted transformations. A variety of acids, N-protected amino acids, acid-containing drugs, and alcohols are all compatible with this reaction. The preliminary simple DG removal and one-step efficient product conversion reaction demonstrate this protocol's potential for structural manipulation to amine-containing diverse functional molecules.

Data availability

All experimental and characterization data in this article are available in the ESI. Crystallographic data for compounds **IN14** have been deposited in the Cambridge Crystallographic Data Centre (CCDC) under accession number CCDC 2058762.†

Author contributions

S. Z. and J. Z. contributed equally. S. Z. and J. Z. conceived the project. S. Z., J. Z. and H. Z. wrote the manuscript.

Conflicts of interest

There are no conflicts to declare.

Acknowledgements

This work was supported by the Key Projects of Natural Science Foundation of Zhejiang Province (LZ21B020001), the National Natural Science Foundation of China (No. 21472170) and the National Key R&D Program of China (No. 2017YFE0102200).

Notes and references

1 (*a*) R. K. Rit, M. R. Yadav and A. K. Sahoo, *Org. Lett.*, 2012, **14**, 3724–3727; (*b*) R. K. Rit, M. R. Yadav and A. K. Sahoo, *Org. Lett.*, 2014, **16**, 968–971; (*c*) D. Li, Y. Cao and G. Wang, *Org. Biomol. Chem.*, 2015, **13**, 6958–6964; (*d*) S. Arshadi, A. Banaei, A. Monfared, S. Ebrahimiasl and A. Hosseinian, *RSC Adv.*, 2019, **9**, 17101–17118.

2 (*a*) B. V. S. Reddy, L. R. Reddy and E. J. Corey, *Org. Lett.*, 2006, **8**, 3391–3394; (*b*) S. Zhang, G. He, Y. Zhao, K. Wright, W. A. Nack and G. Chen, *J. Am. Chem. Soc.*, 2012, **134**, 7313–7316; (*c*) Z. Ren, F. Mo and G. Dong, *J. Am. Chem. Soc.*, 2012, **134**, 16991–16994; (*d*) X. Ye, Z. He, T. Ahmed, K. Weise, N. G. Akhmedov, J. L. Petersen and X. Shi, *Chem. Sci.*, 2013, **4**, 3712–3716; (*e*) Q. Li, S. Zhang, G. He, W. A. Nack and G. Chen, *Adv. Synth. Catal.*, 2014, **356**, 1544–1548; (*f*) Z. Zang, S. Zhao, S. Karnakanti, C. Liu, P. Shao and Y. He, *Org. Lett.*, 2016, **18**, 5014–5017; (*g*) K. K. Pasunooti, R. Yang, B. Banerjee, T. Yap and C. Liu, *Org. Lett.*, 2016, **18**, 2696–2699; (*h*) K. Chen, D. Wang, Z. Li, Z. Liu, F. Pan, Y. Zhang and Z. Shi, *Org. Chem. Front.*, 2017, **4**, 2097–2101; (*i*) Y. Zheng, W. Song, Y. Zhu, B. Wei and L. Xuan, *J. Org. Chem.*, 2018, **83**, 2448–2454; (*j*) K. K. Ghosh, A. Uttry, A. Koldemir, M. Ong and M. van Gemmeren, *Org. Lett.*, 2019, **21**, 7154–7157; (*k*) C. S. Buettner, D. Willcox, B. G. N. Chappell and M. J. Gaunt, *Chem. Sci.*, 2019, **10**, 83–89.

3 (*a*) L. Zhou and W. Lu, *Org. Lett.*, 2014, **16**, 508–511; (*b*) R. Zhao and W. Lu, *Org. Lett.*, 2017, **19**, 1768–1771.

4 Y. Chen, Y. Wu, Z. Wang, J. X. Qiao and J. Yu, *ACS Catal.*, 2020, **10**, 5657–5662.

5 A. J. Canty, M. C. Denney, B. W. Skelton and A. H. White, *Organometallics*, 2004, **23**, 1122–1131.

6 L. V. Desai, K. L. Hull and M. S. Sanford, *J. Am. Chem. Soc.*, 2004, **126**, 9542–9543.

7 R. Giri, J. Liang, J. G. Lei, J. J. Li, D. H. Wang, X. Chen, I. C. Naggar, C. Guo, B. M. Foxman and J. Q. Yu, *Angew. Chem., Int. Ed.*, 2005, **44**, 7420–7424.

8 Z. Zhuang and J. Yu, *Nature*, 2020, **577**, 656–659.

9 Z. Zhuang, A. N. Herron, Z. Fan and J. Yu, *J. Am. Chem. Soc.*, 2020, **142**, 6769–6776.

10 (*a*) P. L. Alsters, H. T. Teunissen, J. Boersma and G. van Koten, *Recl. Trav. Chim. Pays-Bas*, 1990, **109**, 487–489; (*b*) P. L. Alsters, H. T. Teunissen, J. Boersma, A. L. Spek and G. van Koten, *Organometallics*, 1993, **12**, 4691–4696.

11 Y. Zhao and D. G. Truhlar, *Theor. Chem. Acc.*, 2008, **120**, 215–241.

12 F. Weigend and R. Ahlrichs, *Phys. Chem. Chem. Phys.*, 2005, **7**, 3297–3305.

13 (*a*) N. R. Deprez and M. S. Sanford, *J. Am. Chem. Soc.*, 2009, **131**, 11234–11241; (*b*) D. C. Powers, M. A. L. Geibel, J. E. M. N. Klein and T. Ritter, *J. Am. Chem. Soc.*, 2009, **131**, 17050–17051.

14 (*a*) D. G. Blackmond, *Angew. Chem., Int. Ed.*, 2006, **44**, 4302–4320; (*b*) J. S. Mathew, M. Klussmann, H. Iwamura, F. Valera, A. Futran, E. A. C. Emanuelsson and D. G. Blackmond, *J. Org.*

Chem., 2006, **71**, 4711–4722; (*c*) P. Ruiz-Castillo, D. G. Blackmond and S. L. Buchwald, *J. Am. Chem. Soc.*, 2015, **137**, 3085–3092.

15 (*a*) H. Thu, W. Yu and C. Che, *J. Am. Chem. Soc.*, 2006, **128**, 9048–9049; (*b*) Y. Zhang, B. Shi and J. Yu, *Angew. Chem., Int. Ed.*, 2009, **48**, 6097–6100; (*c*) B. E. Haines, H. Xu, P. Verma, X. Wang, J. Yu and D. G. Musaev, *J. Am. Chem. Soc.*, 2015, **137**, 9022–9031.